JACS
JOURNAL OF THE AMERICAN CHEMICAL SOCIETY
pubs.acs.org/JACS
Article

Streamlined Symmetrical Total Synthesis of Disorazole B_1 and Design, Synthesis, and Biological Investigation of Disorazole Analogues

K. C. Nicolaou,* Johannes Krieger, Ganesh M. Murhade, Parthasarathi Subramanian, Balu D. Dherange, Dionisios Vourloumis, Stefan Munneke, Baiwei Lin, Christine Gu, Hetal Sarvaiaya, Joseph Sandoval, Zhaomei Zhang, Monette Aujay, James W. Purcell, and Julia Gavrilyuk

Cite This: https://dx.doi.org/10.1021/jacs.0c07094
Read Online

ABSTRACT: Taking advantage of the C_2-symmetry of the antitumor naturally occurring disorazole B_1 molecule, a symmetrical total synthesis was devised with a monomeric advanced intermediate as the key building block, whose three-step conversion to the natural product allowed for an expeditious entry to this family of compounds. Application of the developed synthetic strategies and methods provided a series of designed analogues of disorazole B_1, whose biological evaluation led to the identification of a number of potent antitumor agents and the first structure−activity relationships (SARs) within this class of compounds. Specifically, the substitutions of the epoxide units and lactone moieties with cyclopropyl and lactam structural motifs, respectively, were found to be tolerable for biological activities and beneficial with regard to chemical stability.

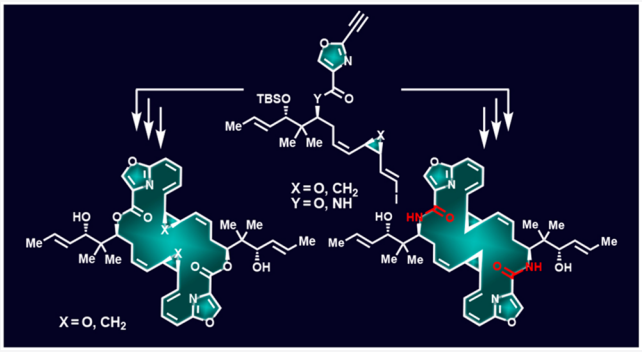

1. INTRODUCTION

Comprising numerous synthetically challenging natural products, the disorazole family of compounds[1] attracted the interest of synthetic organic chemists and biologists alike due to their novel molecular structures and potent antitumor properties.[2] We recently reported the first total syntheses of disorazoles A_1 (**1**, Figure 1) and B_1 (**2**, Figure 1) and assigned the full stereochemical structure of the latter,[3] whose epoxide configurations were previously unknown.[1a] We also subsequently disclosed the application of our developed modular synthetic strategies toward these natural products to the synthesis of the corresponding biscyclopropyl and bisthiazolyl analogues of both disorazoles A_1 (**1**) and B_1 (**2**), including biscyclopropyl disorazole B_1 (**3**, Figure 1).[4] In this article we report a streamlined, symmetrical total synthesis of disorazole B_1 (**2**) and its application to, in addition to the previously reported biscyclopropyl disorazole B_1 (**3**), several new analogues (i.e., **4**−**12**, Figure 2), and their biological evaluation and that of the parent compound disorazole B_1 (**2**), as antitumor agents.

2. RESULTS AND DISCUSSION

Our first objective was to develop a more efficient route to disorazole B_1 (**2**) than our first total synthesis now based on a symmetrical and more convergent synthetic strategy, taking advantage of the C_2-symmetrical structure of the molecule.[5] Such an approach was expected to be considerably shorter than our previous nonsymmetrical approach that required the construction of two advanced intermediates reached through multistep sequences, as opposed to our new strategy that would require only one advanced intermediate, whose dimerization−cyclization would lead directly to the required macrocyclic precursor of the targeted molecules. Furthermore, our new strategy avoids the facile isomerization of certain olefinic bonds of the conjugated structural motifs of the precyclization intermediates by replacing the vulnerable double bonds with acetylenic units until after cyclization, when they can be safely converted to their desired (*Z*)-olefinic bonds through Lindlar hydrogenation.

Figure 2 depicts the designed disorazole B_1 analogues (**4**−**12**) synthesized in this study, applying the newly developed symmetrical total synthesis of disorazole B_1. The design of these analogues was based on the following rationales: (a) the synthetic strategy employed (e.g., involvement of bisacetylene

Received: July 1, 2020

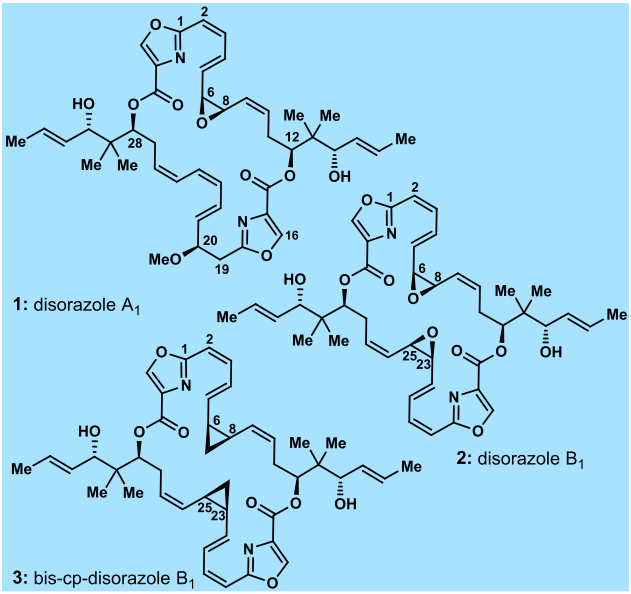

Figure 1. Molecular structures of disorazole A_1 (**1**), B_1 (**2**), and biscyclopropyl disorazole B_1 (**3**).

advanced precursors); (b) the expected stability of the biscyclopropyl structural motifs (as opposed to the more labile epoxide structural motifs); (c) the opportunity to explore substituents on the lipophilic side-chain residues and oxazole moieties of disorazoles B_1 (biological evaluation); and (d) the inspiring success of the clinically used anticancer drug Ixabepilone[6] (containing the macrolactam structural motif as opposed to the macrolactone of its parent natural product epothilone B).

2.1. Streamlined Symmetrical Total Synthesis of Disorazole B_1 (2). Figure 3 summarizes, in retrosynthetic format, our original nonsymmetrical approach to disorazole B_1 (**2**, Figure 3A) through intermediate **13** and our proposed symmetrical approach based on a Sonogashira coupling/macrocyclization (Figure 3B).[7] The construction of required building blocks **14** and **15** (Figure 3A) required numerous steps and then stepwise coupling (to afford **13**) and macrolactonization. In contrast, the new symmetrical approach (Figure 3B) required building blocks iodide **18**,[3,4] aldehyde **19**, and acetylene carboxylic acid **20** to be assembled into key advanced intermediate **17**, whose palladium−copper-catalyzed Sonogashira coupling/macrocyclization, followed by sequential selective Lindlar hydrogenation and deprotection, was expected to afford disorazole B_1 (**2**), via bisacetylene precursor **16**, in a shorter and streamlined way, as outlined in Figure 3B.

Scheme 1 depicts the construction of the defined building blocks **19** (Scheme 1A) and **20** (Scheme 1B) and their sequential coupling with our previously synthesized iodide building block **18**[3,4] and elaboration to disorazole B_1 (**2**) (Scheme 1C). Thus, commercially available acetylene diethoxyacetal **21** was treated with NaI in the presence of H_2SO_4 to afford the corresponding vinyl iodide aldehyde, which was reacted with the anion of the commercially available methyl ester phosphonate **22** (KHMDS, 18-crown-6) to afford selectively (*Z*,*E*)-methyl ester iodide **23** (78% overall yield). The latter was reduced with DIBAL-H to the corresponding allylic alcohol, whose Sharpless epoxidation [TBHP, Ti(O*i*Pr)$_4$, (−)-DET] furnished the expected epoxide **25** as the major enantiomer as

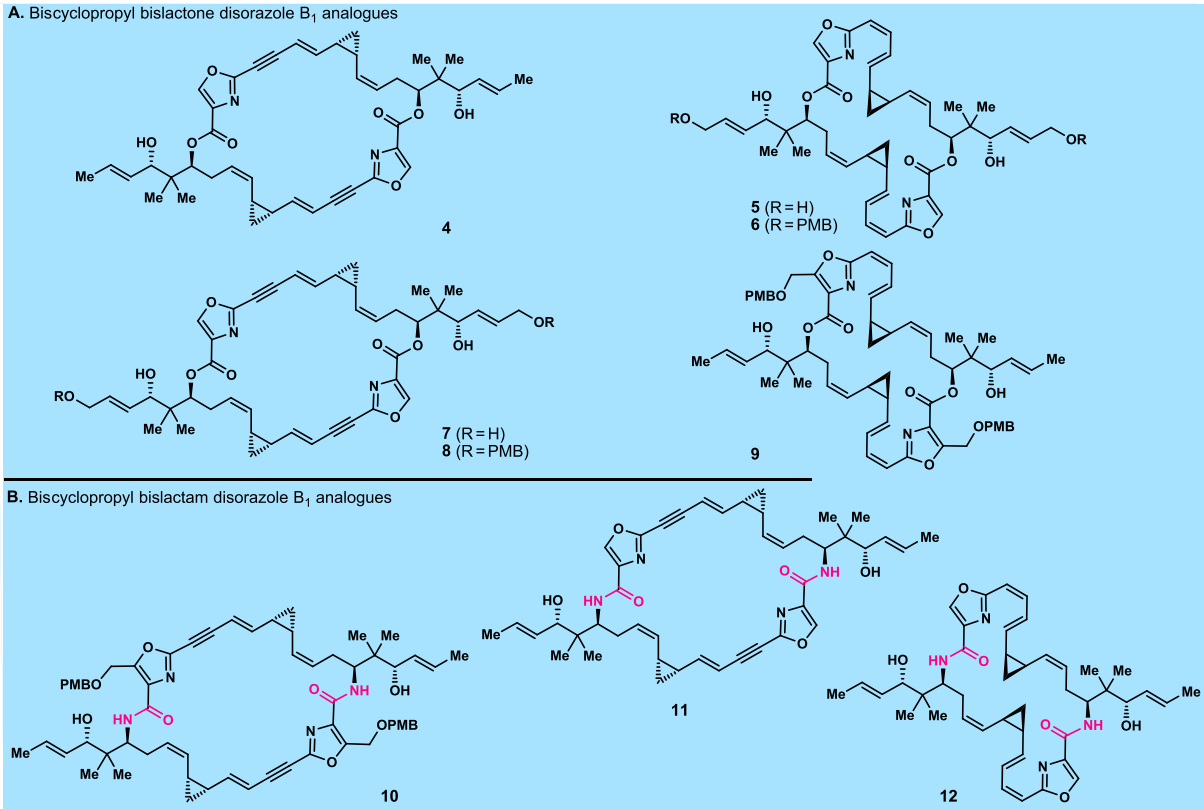

Figure 2. Molecular structures of designed and synthesized disorazole B_1 analogues **4**−**12**. (A) Biscyclopropyl bislactone analogues. (B) Biscyclopropyl bislactam analogues. PMB = *para*-methoxybenzyl.

https://dx.doi.org/10.1021/jacs.0c07094
J. Am. Chem. Soc. XXXX, XXX, XXX−XXX

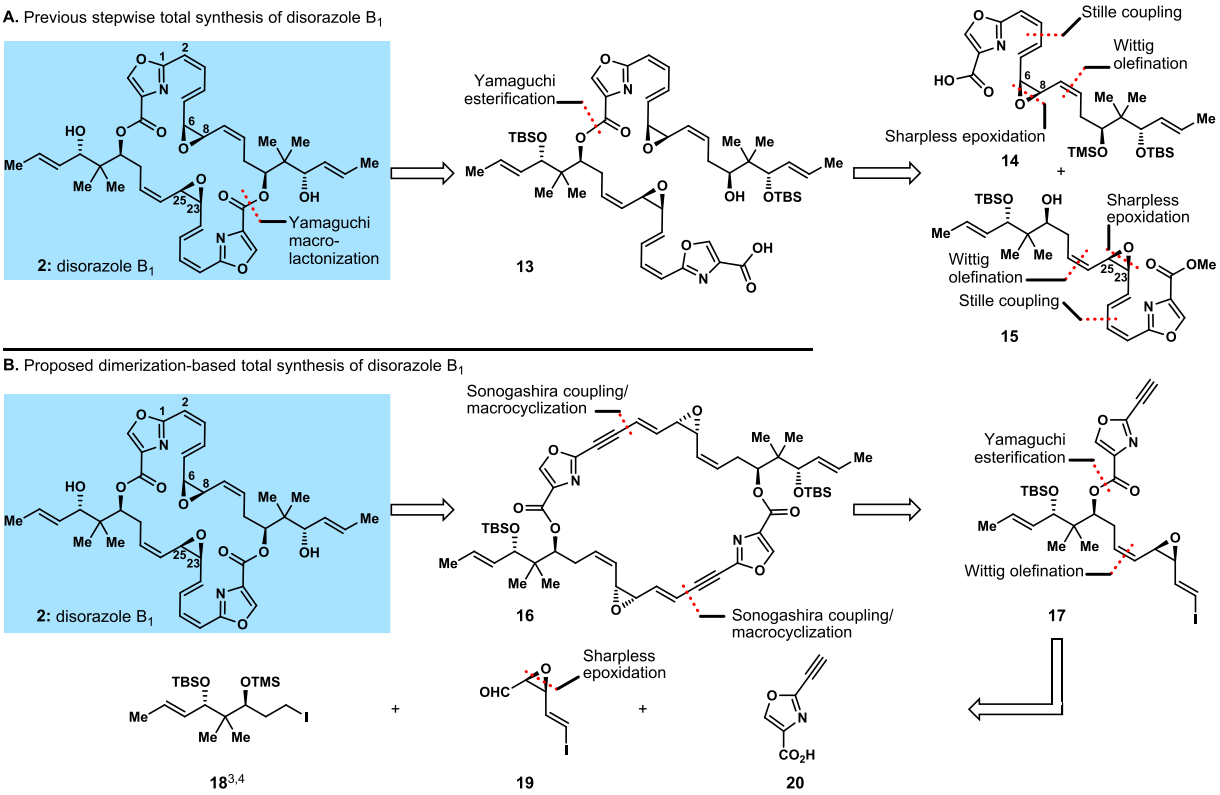

Figure 3. Retrosynthetic analyses of disorazole B_1 (**2**). (A) Previously developed[3] stepwise macrolactonization approach. (B) Proposed streamlined symmetrical Sonogashira dimerization/cyclization approach. TMS = trimethylsilyl; TBS = *tert*-butyldimethylsilyl.

theoretically predicted [(−)-DET-facilitated *Si* face attack of the allyl alcohol double bond (61% overall yield from **23**)], as shown in Scheme 1A. The enantiomeric excess of the latter was enriched through kinetic resolution by exposure to vinyl acetate and Amano lipase PS, with the undesired enantiomer (**24**, see Scheme 1A) being removed chromatographically as the acetate derivative (76% yield for **25**). DMP oxidation of intermediate epoxy alcohol (**25**) then gave the desired aldehyde **19** (55% yield). Due to the rather labile nature of this aldehyde and its precursor allylic alcohol **25**, these intermediates were rushed through the sequence (i.e., epoxidation, Amano lipase PS kinetic resolution, oxidation, and Wittig olefination). The absolute configurations of **25** and **19** were confirmed at a later stage as we shall discuss below.

The required acetylene carboxylic acid **20** was prepared from commercially available oxazole ethyl ester **26** as shown in Scheme 1B. Thus, oxazole **26** was lithiated (LHMDS), and the resulting lithio derivative was quenched with 1,2-diiodoethane to afford iodo oxazole **27** (51% yield), whose palladium/copper-catalyzed coupling with TIPS-acetylene led to oxazole acetylene **28** (75% yield). Sequential deprotection of **28** (TBAF, 86% yield; then LiOH, 99% yield) furnished the desired building block acetylene carboxylic acid **20**, as shown in Scheme 1B.

With both fragments **19** and **20** readily available, their assembly with previously synthesized fragment **18**[3,4] proceeded as summarized in Scheme 1C. Thus, iodide **18** was converted to its phosphonium salt (PPh_3, *i*-Pr_2NEt), which underwent Wittig olefination with epoxy aldehyde **19** as facilitated with ylide formation (LHMDS, DMPU) to afford epoxy vinyl iodide **29** (64% yield for the two steps). The latter (**29**, more stable as opposed to the labile aldehyde **19** and its precursor alcohol **25**) was transformed to the key monomeric building block **17** by sequential selective TMS removal (3HF·Et_3N, 73% yield) and esterification of the resulting hydroxy intermediate with carboxylic acid acetylene **20** [2,4,6-trichlorobenzoyl chloride (TCBC), Et_3N, DMAP, 92% yield] as depicted in Scheme 1C. Exposure of vinyl iodide terminal acetylene **17** to $Pd(PPh_3)_4$ cat. in the presence of stochiometric CuI furnished macrocycle **16** (40% yield) through coupling and macrocyclization. The latter was selectively reduced with H_2 under Lindlar conditions in the presence of quinoline to afford bis-TBS disorazole B_1 (**30**, 70% yield), whose desilylation (TASF, 78% yield) furnished the coveted natural product disorazole B_1 (**2**). Ultimate precursor **30** and synthetic disorazole B_1 (**2**) exhibited identical physical data to those previously observed in our first total synthesis,[3] thereby confirming the absolute configurations of building block **19** and its precursor **25** (Scheme 1A). This symmetrical total synthesis of disorazole B_1 (**2**) proceeded in 17 total number of steps and in 3% overall yield (12 steps longest linear sequence from **21**) from readily available building blocks **21**, **26**, and **18**,[3,4] as opposed to our first total synthesis, which required a total of 29 steps and gave the desired natural product in 1.8% overall yield (15 steps longest linear sequence) starting from propargyl alcohol.[3]

2.2. Synthesis of Disorazole B_1 Analogues 3−9. The synthetic strategy for the streamlined total synthesis of disorazole B_1 analogues **3** (biscyclopropyl disorazole B_1) and **4** (biscyclopropyl bisacetylene disorazole B_1) was derived from the retrosynthetic analysis indicated in Scheme 2A. Requiring key building blocks **18**,[3,4] **20** (Scheme 1B), and **33** and proceeding through advanced monomeric precursor iodo acetylene **32**, the total synthesis of these analogues proceeded as summarized in Scheme 2. While intermediates **20** (Scheme 1B) and **18**[3,4] were available to us from our earlier studies, the

https://dx.doi.org/10.1021/jacs.0c07094
J. Am. Chem. Soc. XXXX, XXX, XXX−XXX

Scheme 1. Streamlined Total Synthesis of Disorazole B_1[a]

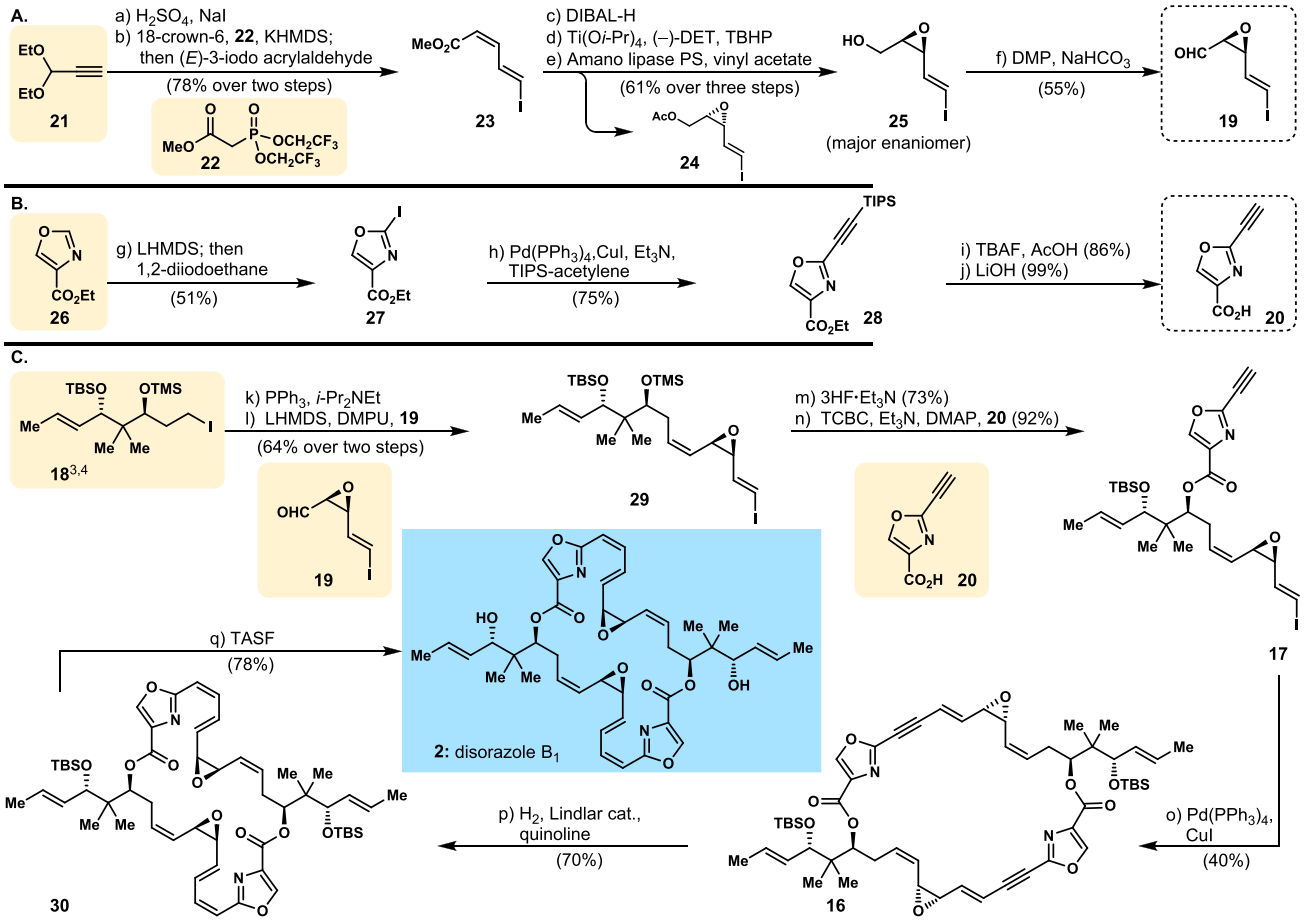

[a]Reagents and conditions: (a) 4 M aq. H_2SO_4:Et_2O (1:1, *v*/*v*), NaI (1.5 equiv), 0 °C, 20 h; (b) 18-crown-6 (4.0 equiv), **22** (1.2 equiv), KHMDS (1.1 equiv), −78 °C, 5 min; then (*E*)-3-iodo acrylaldehyde, −78 °C, 0.5 h, 78% over two steps; (c) DIBAL-H (2.2 equiv), Et_2O, −78 to 0 °C, 2 h; (d) TBHP (2.0 equiv), Ti(O*i*-Pr)$_4$ (0.10 equiv), (−)-DET (0.15 equiv), 3 Å molecular sieves, CH_2Cl_2, −78 to −20 °C, 16 h, 80% over two steps; (e) Amano lipase PS, vinyl acetate, CH_2Cl_2, 0 °C, 16 h, 76%; (f) DMP (1.2 equiv), $NaHCO_3$ (4.0 equiv), CH_2Cl_2, 0 °C, 2 h, 55%; (g) LHMDS (1.5 equiv), THF, −78 °C, 1 h; then 1,2-diiodoethane (1.2 equiv), −78 to −20 °C, 5 h, 51%; (h) TIPS-acetylene (3.0 equiv), CuI (0.06 equiv), Pd(PPh$_3$)$_4$ (0.03 equiv), DMF:Et_3N (1:1, *v*/*v*), 60 °C, 16 h, 75%; (i) TBAF (1.3 equiv), AcOH (4.0 equiv), THF, 0 °C, 2 h, 86%; (j) LiOH·H_2O (2.0 equiv), dioxane:H_2O (4:1, *v*/*v*), 23 °C, 16 h, 99%; (k) **18** (1.2 equiv), PPh_3 (1.9 equiv), *i*-Pr_2NEt, 90 °C, 20 h; (l) LHMDS (1.2 equiv), THF, −78 °C, 0.5 h; then DMPU (0.7 equiv), −78 °C, 15 min; then **19** (1.0 equiv), −78 to 23 °C, 8 h, 64% two steps [(*Z*):(*E*) ca. 6:1]; (m) 3HF·Et_3N (1.7 equiv), THF, 23 °C, 3 h, 73%; (n) **20** (2.0 equiv), Et_3N (4.0 equiv), DMAP (4.0 equiv), TCBC (2.0 equiv), toluene, 23 °C, 3 h, 92%; (o) CuI (1.0 equiv), Pd(PPh$_3$)$_4$ (0.25 equiv), DMF:Et_3N (2:1, *v*/*v*), 0 °C, 6 h, 40%; (p) Lindlar cat., quinoline, H_2, ethyl acetate, 23 °C, 1 h, 70%; (q) TASF, H_2O, DMF, 45 °C, 48 h, 78%. KHMDS = potassium 1,1,1-trimethyl-*N*-(trimethylsilyl)silanaminide; LHMDS = lithium 1,1,1-trimethyl-*N*-(trimethylsilyl)silanaminide; DMPU = 1,3-dimethyl-1,3-diazinan-2-one; DIBAL-H = diisobutylaluminum hydride; DET = diethyl 2,3-dihydroxybutanedioate; TBHP = 2-methylpropane-2-peroxol; DMP = Dess−Martin periodinane; TIPS = triisopropylsilyl; TBAF = tetra-*n*-butylammonium fluoride; TCBC = 2,4,6-trichlorobenzoyl chloride; DMAP = *N*,*N*-dimethylpyridin-4-amine; TASF = tris(dimethylamino)-sulfonium difluorotrimethylsilicate.

requisite iodo aldehyde **33** was prepared from readily available allylic alcohol **34**[8] through the dual path shown in Scheme 2B. Thus, **34** was subjected to cyclopropanation (CH_2I_2, $ZnEt_2$) to afford hydroxy cyclopropyl diastereoisomers **35** and **36** [72% yield, **35** (path a):**36** (path b) ca. 1:6.2 dr]. The desired diastereoisomer **35**, whose absolute configuration was established by comparison of its spectroscopic and optical rotation data to those of the previously synthesized material,[8b] was converted to vinyl iodide **37** [(*E*):(*Z*) ca. 4.5:1 dr] by sequential DMP oxidation (94% yield) to the corresponding aldehyde and reaction of the latter with CH_2I_2 and $CrCl_2$ (67% yield). The targeted (*E*)-vinyl iodide **33** was then prepared from the (*E*/*Z*)-mixture of **37** through sequential deprotection (*p*-TsOH, H_2O, 99% yield) and cleavage of the so-formed 1,2-diol ($NaIO_4$, 75% yield) followed by chromatographic purification, as shown in Scheme 2B (path a). The other, chromatographically separated diastereoisomer **36** was transformed to the same desired fragment **33** through path b, as summarized in Scheme 2B. Thus, PMB protection of the hydroxyl group within **36** (**38**, PPTS cat.), followed by acetonide cleavage (aq. HCl), afforded dihydroxy PMB-ether **39** in 86% overall yield. The 1,2-diol moiety of the latter was cleaved ($NaIO_4$, 84% yield), and the resulting aldehyde was subjected to Takai olefination (CHI_3, $CrCl_2$, 63% yield) to yield iodo olefin **40** [(*E*):(*Z*) ca. 4.6:1], as shown in Scheme 2B (path b). Removal of the PMB protecting group (DDQ, 98% yield) from **40** and DMP oxidation (78% yield) of the resulting primary alcohol gave, after chromatographic separation, the same cyclopropyl iodo aldehyde fragment **33** (78% yield) as the one obtained via path a (Scheme 2B).

https://dx.doi.org/10.1021/jacs.0c07094
J. Am. Chem. Soc. XXXX, XXX, XXX−XXX

Scheme 2. Synthesis of Disorazole B_1 Analogues 3 and 4[a]

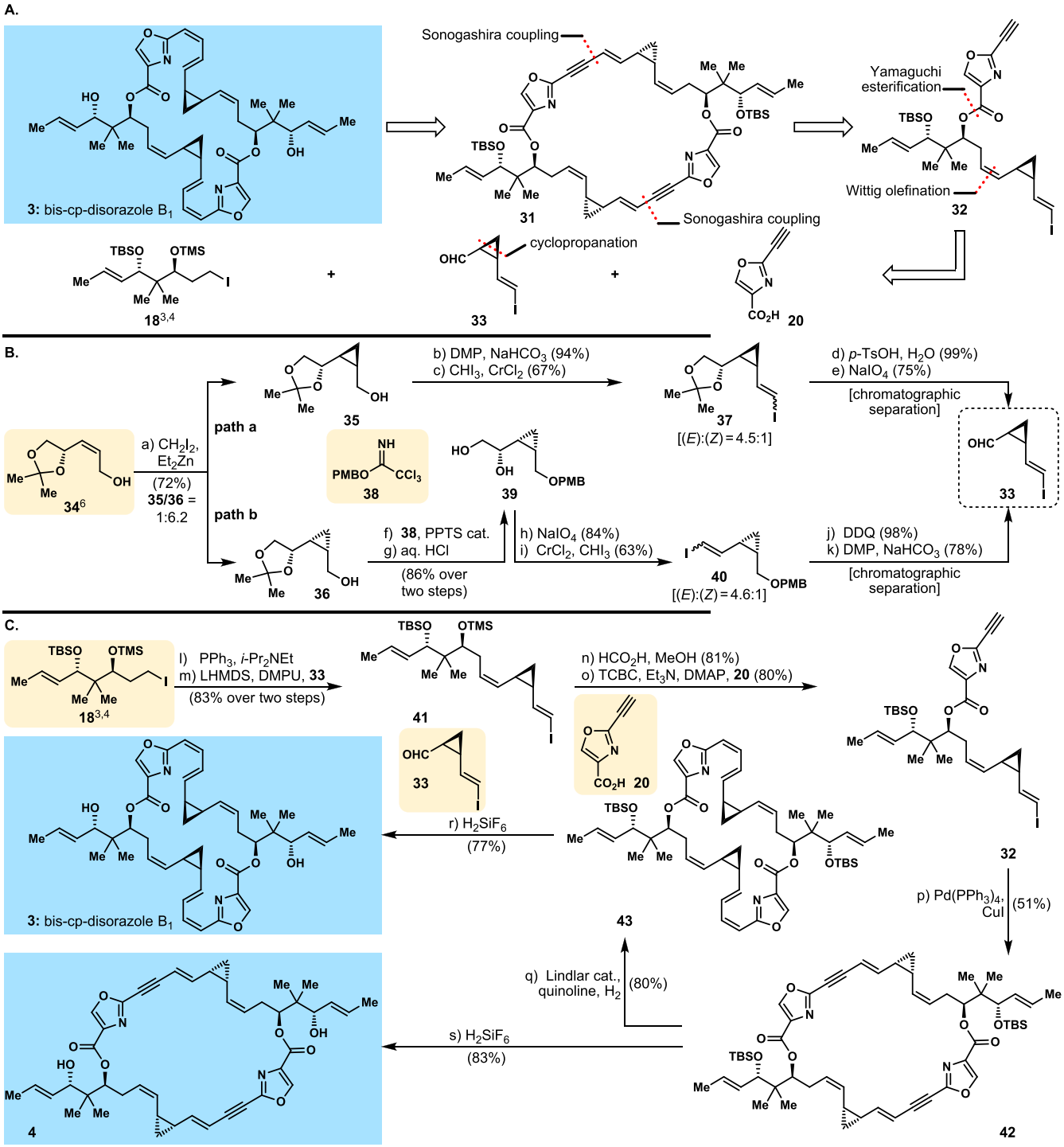

[a]Reagents and conditions: (a) CH_2I_2 (4.0 equiv), Et_2Zn (2.1 equiv), CH_2Cl_2, 0 °C, 1 h; then **34** (1.0 equiv), 0 to 23 °C, 12 h, 10% for **35**; 62% for **36**; (b) DMP (1.25 equiv), $NaHCO_3$ (3.0 equiv), CH_2Cl_2, 23 °C, 2 h, 94%; (c) $CrCl_2$ (7.0 equiv), CHI_3 (2.0 equiv), THF, 0 °C, 3 h, 67% [(*E*)/(*Z*) = 4.5:1)]; (d) *p*-TsOH·H_2O (0.1 equiv), THF:H_2O (4:1, *v*/*v*), 45 °C, 24 h, 99%; (e) $NaIO_4$ (2.0 equiv), CH_2Cl_2:H_2O:aq. $NaHCO_3$ (2:1:1, *v*/*v*/*v*), 23 °C, 3 h, 75%; (f) **38** (1.3 equiv), PPTS (0.05 equiv), CH_2Cl_2, 23 °C, 16 h; (g) THF:4 M aq. HCl (4:1, *v*/*v*), 23 °C, 3 h, 86% over two steps; (h) $NaIO_4$ (1.75 equiv), CH_2Cl_2:H_2O:aq. $NaHCO_3$ (2:1:1, *v*/*v*/*v*), 23 °C, 3 h, 84%; (i) $CrCl_2$ (7.0 equiv), CHI_3 (2.0 equiv), THF, 0 °C, 2 h, 63% [(*E*):(*Z*) = 4.6:1]; (j) DDQ (1.75 equiv), CH_2Cl_2:pH 7 buffer (20:1, *v*/*v*), 23 °C, 1 h, 98%; (k) DMP (1.2 equiv), $NaHCO_3$ (3.0 equiv), CH_2Cl_2, 23 °C, 2 h, 78%; (l) PPh_3 (1.75 equiv), *i*-Pr_2NEt, 90 °C, 20 h; (m) LHMDS (1.05 equiv), THF, −78 °C, 0.5 h; then DMPU (0.6 equiv), −78 °C, 15 min; then **33** (1.0 equiv), −78 to 23 °C, 8 h, 83% over two steps; (n) HCO_2H (3.0 equiv), MeOH, 0 °C, 2 h, 81%; (o) **20** (1.5 equiv), Et_3N (3.0 equiv), DMAP (4.0 equiv), TCBC (2.0 equiv), toluene, 23 °C, 3 h, 80%; (p) CuI (0.40 equiv), $Pd(PPh_3)_4$ (0.2 equiv), DMF:Et_3N (2:1, *v*/*v*), 23 °C, 16 h, 51%; (q) Lindlar cat., quinoline, H_2, ethyl acetate, 23 °C, 3 h, 80%; (r) H_2SiF_6 (75 equiv), MeOH, 23 °C, 48 h, 77%; (s) H_2SiF_6 (75 equiv), MeOH, 23 °C, 48 h, 83%.

https://dx.doi.org/10.1021/jacs.0c07094
J. Am. Chem. Soc. XXXX, XXX, XXX−XXX

Scheme 3. Synthesis of Disorazole B_1 Analogues 5−8[a]

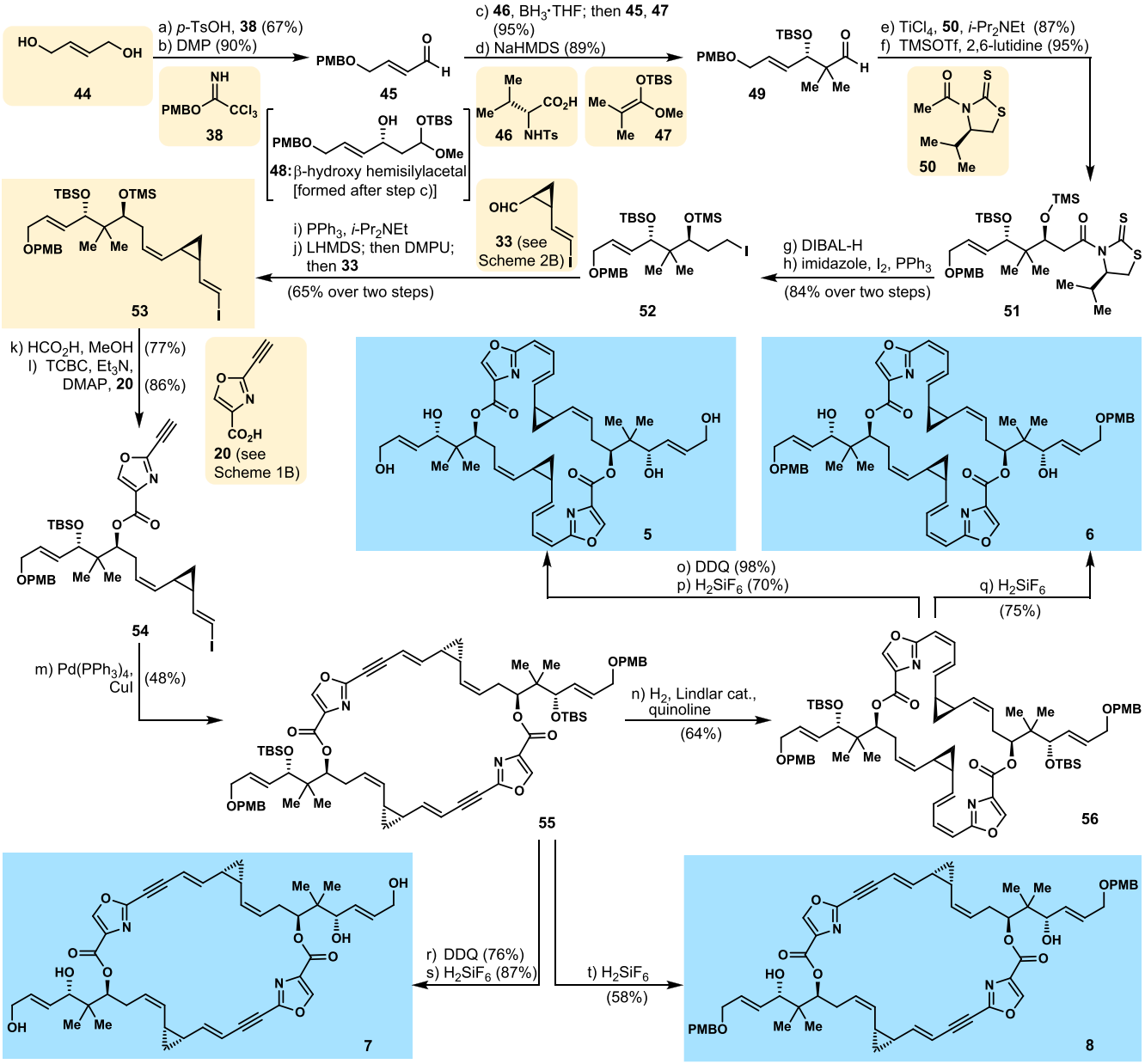

[a]Reagents and conditions: (a) **44** (2.0 equiv), *p*-TsOH (0.05 equiv), **38** (1.1 equiv), 23 °C, 24 h, 67%; (b) DMP, CH_2Cl_2, 23 °C, 2 h, 90%; (c) BH_3·THF (1.05 equiv), **46** (1.1 equiv), CH_2Cl_2, 0 to 23 °C, 1.5 h; then cooled to −78 °C, **45** (1.0 equiv), **47** (1.15 equiv), 2 h, 95%; (d) NaHMDS (1.1 equiv), THF, −78 to 23 °C, 89%; (e) $TiCl_4$ (1.6 equiv), CH_2Cl_2, 0 °C, 10 min; then −78 °C, *i*-Pr_2NEt (1.2 equiv), 0.5 h; then −50 °C; 2 h; then −78 °C, **49** (1.0 equiv), 1 h, 87%; (f) TMSOTf (1.05 equiv), 2,6-lutidine (2.5 equiv), CH_2Cl_2, 0 °C, 1 h, 95%; (g) DIBAL-H, Et_2O, −78 to 23 °C, 2 h; (h) imidazole (1.5 equiv), PPh_3 (1.2 equiv), I_2 (1.35 equiv), CH_2Cl_2, 0 °C, 1 h; 84% over two steps; (i) PPh_3 (1.75 equiv), *i*-Pr_2NEt, 90 °C, 20 h; (j) LHMDS (1.05 equiv), THF, −78 °C, 0.5 h; then DMPU (0.6 equiv), −78 °C, 15 min; then **33** (1.0 equiv), −78 to 23 °C, 8 h, 65% over two steps; (k) HCO_2H (3.0 equiv), MeOH, 0 °C, 2 h, 77%; (l) **20** (2.0 equiv), Et_3N (4.0 equiv), DMAP (4.0 equiv), TCBC, (2.0 equiv), toluene, 0 to 23 °C, 5 h, 86%; (m) CuI (1.0 equiv), $Pd(PPh_3)_4$ (0.25 equiv), DMF:Et_3N (2:1, *v*/*v*), 0 to 23 °C, 12 h, 48%; (n) Lindlar catalyst, quinoline, H_2, ethyl acetate, 23 °C, 8 h, 64%; (o) DDQ (4.0 equiv), CH_2Cl_2:pH 7 buffer (40:1, *v*/*v*), 23 °C, 3 h, 98%; (p) H_2SiF_6 (75 equiv), MeOH, 23 °C, 36 h, 70%; (q) H_2SiF_6 (75 equiv), MeOH, 23 °C, 48 h, 75%; (r) DDQ (4.0 equiv), CH_2Cl_2:pH 7 buffer (40:1, *v*/*v*), 23 °C, 3 h, 76%; (s) H_2SiF_6 (75 equiv), MeOH, 23 °C, 36 h, 87%; (t) H_2SiF_6 (75 equiv), MeOH, 23 °C, 48 h, 58%. *p*-TSA = 4-methylbenzene-1-sulfonic acid; TMSOTf = trimethylsilyl trifluoromethanesulfonate; DDQ = 4,5-dichloro-3,6-dioxocyclohexa-1,4-diene-1,2-dicarbonitrile.

With all three building blocks (i.e., **18**, **20**, and **33**) now available, the synthesis of targeted analogues **3** and **4** was completed through the short pathway shown in Scheme 2C. Thus, iodide **18**[3,4] was converted to its phosphonium salt (PPh_3, *i*-Pr_2NEt), which was reacted with LHMDS in the presence of DMPU and aldehyde **33** to afford (*Z*)-olefin **41** (83% overall yield). The TMS protecting group was removed from the latter (HCO_2H, 81% yield), and the intermediate hydroxy compound was esterified with acetylene carboxylic acid fragment **20** (TCBC, Et_3N, DMAP, 80% yield) to yield the targeted monomeric vinyl iodide acetylene **32**. The latter underwent dimerization/macrocyclization through a two-step sequential reaction [$Pd(PPh_3)_4$ cat., CuI cat.] to give biscyclopropyl bisacetylene macrocycle **42** in 51% yield. The latter served well

https://dx.doi.org/10.1021/jacs.0c07094
J. Am. Chem. Soc. XXXX, XXX, XXX−XXX

Scheme 4. Synthesis of Disorazole B_1 Analogue 9[a]

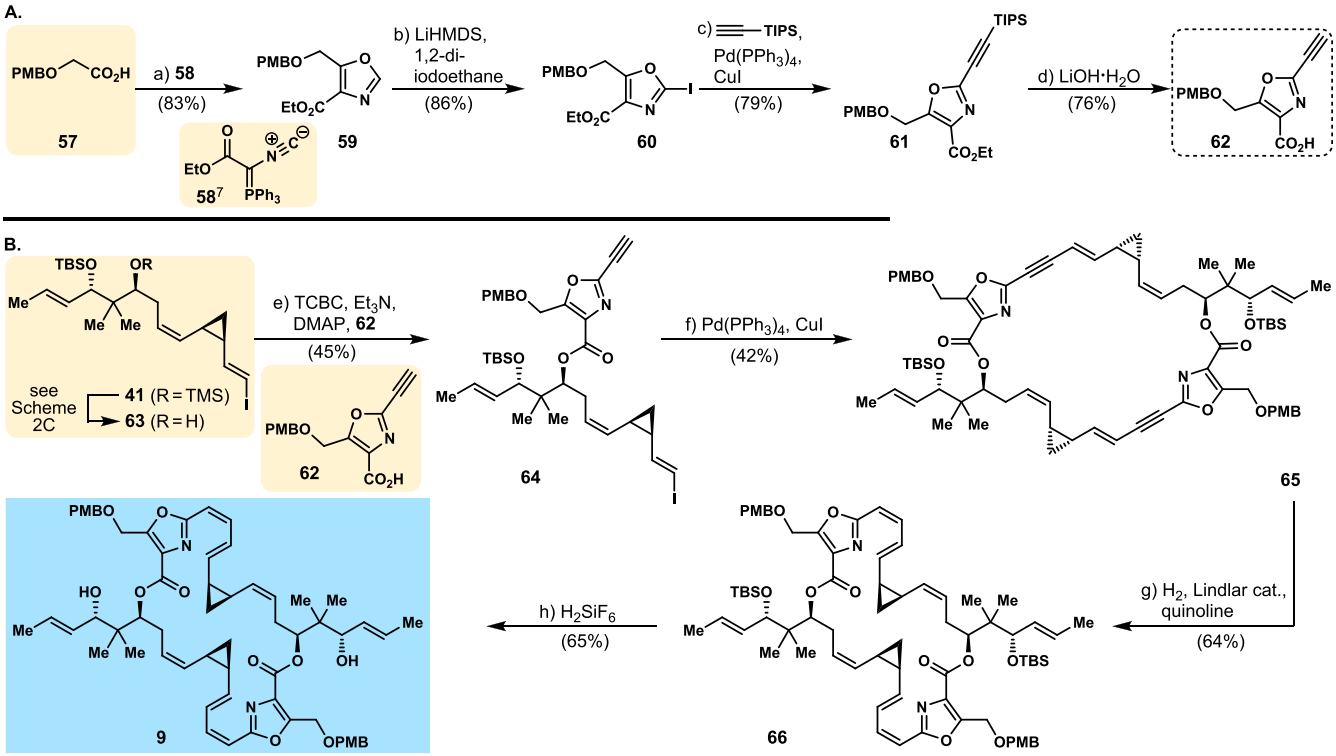

[a]Reagents and conditions: (a) **58**[10] (1.05 equiv), CH_2Cl_2, 23 °C, 12 h, 83%; (b) LiHMDS (1.5 equiv), 1,2-diiodoethane (1.2 equiv), THF, −78 to 23 °C, 12 h, 86%; (c) triisopropylsilylacetylene (3.0 equiv), $Pd(PPh_3)_4$ (0.03 equiv), CuI (0.06 equiv), DMF:Et_3N (1:1, *v*/*v*), 60 °C, 10 h, 79%; (d) LiOH·H_2O (3.0 equiv), THF:H_2O (3:1, *v*/*v*), 23 °C, 4 h, 76%; (e) **62** (2.0 equiv), Et_3N (4.0 equiv), DMAP (4.0 equiv), TCBC, (2.0 equiv), toluene, 0 to 23 °C, 3 h, 45%; (f) CuI (1.0 equiv), $Pd(PPh_3)_4$ (0.25 equiv), DMF:Et_3N (2:1, *v*/*v*), 0 to 23 °C, 12 h, 42%; (g) Lindlar catalyst, quinoline, H_2, ethyl acetate, 23 °C, 8 h, 64%; (h) H_2SiF_6 (75 equiv), MeOH, 23 °C, 48 h, 65%.

as a precursor to the coveted biscyclopropyl disorazole B_1 analogue **3** as achieved through a two-step sequence, via intermediate **43**, involving Lindlar hydrogenation (H_2, Lindlar cat., quinoline, 80% yield), followed by desilylation (H_2SiF_6, 77% yield), as shown in Scheme 2C. Biscyclopropyl bisacetylene analogue **4** was directly generated from precursor **42** upon exposure to H_2SiF_6, in 83% yield, as summarized in Scheme 2C.

Scheme 3 summarizes the total synthesis of dehydroxylated biscyclopropyl disorazole B_1 analogues **5**−**8**. The common advanced precursor **55** was defined through retrosynthetic analysis that involved a divergent approach to all four targeted analogues and defined as key fragments **20** (see Scheme 1B for preparation) and **53**, whose construction and further elaboration to the targeted compounds are shown in Scheme 3. Thus, starting with readily available diol **44**, PMB α,β-unsaturated aldehyde **45** was prepared through reaction with benzylating reagent **38** in the presence of *p*-TsOH cat. (67% yield of mono PMB ether), followed by oxidation of the remaining hydroxyl group (DMP, 90% yield). Reaction of aldehyde **45**, first with the chiral borane reagent [prepared in situ from BH_3·THF and *N*-tosyl-D-valine (**46**)] and subsequently with ketene silyl acetal **47**, followed by treatment of the resulting β-hydroxy hemisilylacetal (see structure **48** in brackets in Scheme 3, 95% yield) with NaHMDS (inducing migration of the TBS group and collapse of the acetal) furnished, enantioselectively, extended fragment aldehyde **49** in 89% yield. Addition of aldehyde **49** to the anion generated from Nagao auxiliary **50**[9] and *i*-Pr_2NEt in the presence of $TiCl_4$ gave, stereoselectively, the corresponding hydroxy compound (87% yield), which was silylated (TMSCl, 2,6-lutidine) leading to intermediate **51** (95% yield), as shown in Scheme 3. Treatment of the latter with DIBAL-H, followed by exposure of the so-formed alcohol to I_2 and PPh_3 in the presence of imidazole, gave iodide **52** (84% overall yield from **51**). Conversion of iodide **52** to its phosphonium salt (PPh_3, *i*-Pr_2NEt), followed by ylide formation (LHMDS) and sequential addition of DMPU and iodo aldehyde **33**, led to fragment **53** stereoselectively and in 65% overall yield, as depicted in Scheme 3. Selective removal of the TMS group from the latter (HCOOH, 77% yield), followed by esterification (TCBC, Et_3N, DMAP) of the so-generated alcohol with carboxylic acid **20**, afforded the coveted vinyl iodide acetylene fragment **54**, in 86% yield as depicted in Scheme 3. This monomeric precursor was then subjected to the palladium/copper dimerization/macrocyclization [$Pd(PPh_3)_4$ cat., CuI, 48% yield] to give bisacetylene diolide precursor **55**, which was transformed selectively to the next polyunsaturated precursor **56** through hydrogenation with Lindlar catalyst in the presence of quinoline in 64% yield, as shown in Scheme 3. Precursor **56** gave rise to targeted tetrahydroxy analogue **5** after sequential exposure, first to DDQ (98% yield) and then H_2SiF_6 (70% yield), and bishydroxy bis-PMB analogue **6** upon treatment with H_2SiF_6 (75% yield), as summarized in Scheme 3. Similarly, bisacetylene precursor **55** was converted to tetrahydroxy analogue **7** through a two-step sequence involving removal of the PMB protecting groups (DDQ, 76% yield) followed by cleavage of the TBS groups (H_2SiF_6, 87% yield) and to bis-PMB dihydroxy analogue **8** by exposure to H_2SiF_6 (58% yield), as shown in Scheme 3.

https://dx.doi.org/10.1021/jacs.0c07094
J. Am. Chem. Soc. XXXX, XXX, XXX−XXX

Scheme 5. Synthesis of Bislactam Disorazole B_1 Analogues 10−12[a]

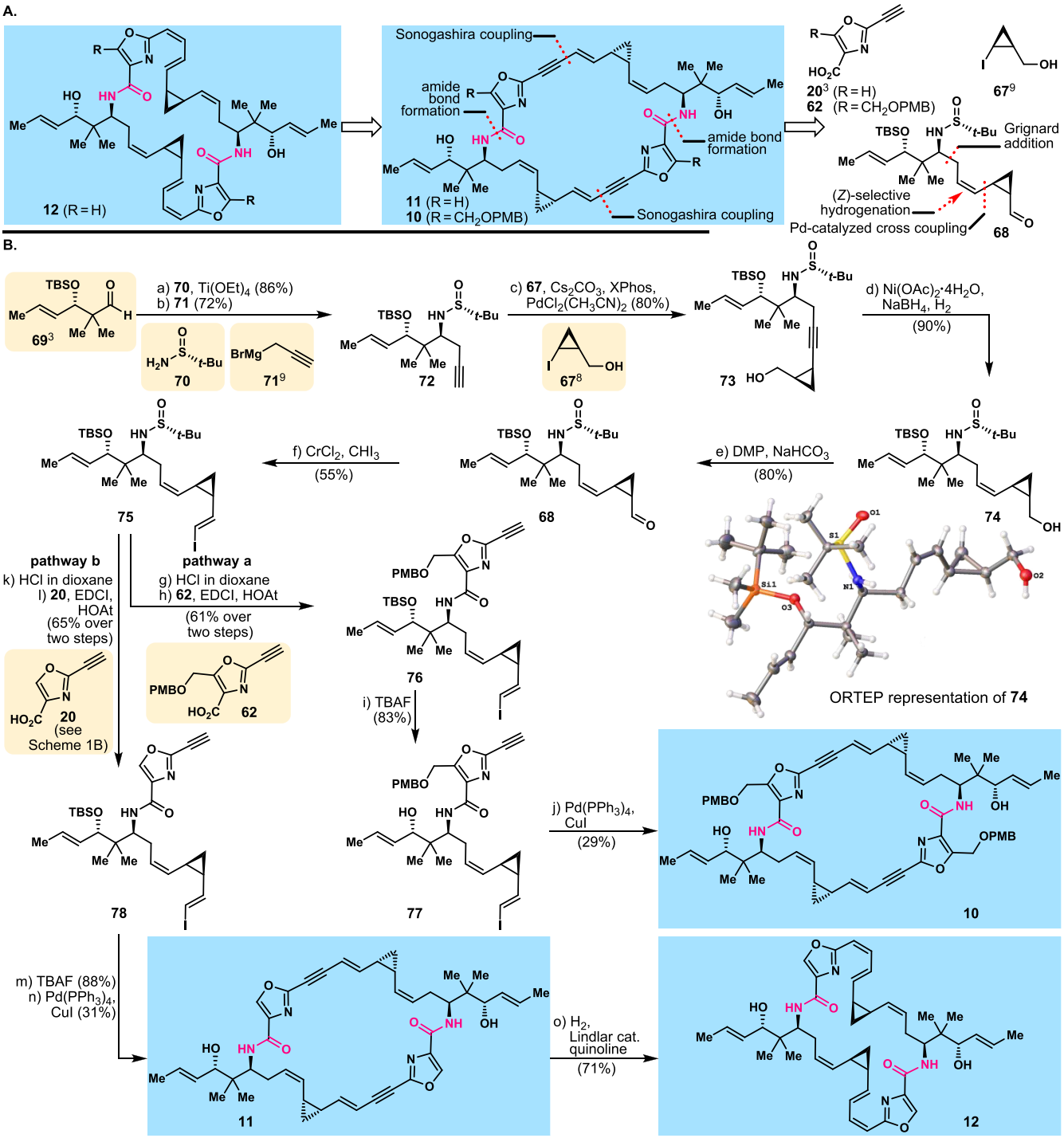

[a]Reagents and conditions: (a) **70** (1.0 equiv), $Ti(OEt)_4$ (2.0 equiv), CH_2Cl_2, 0 to 23 °C, 12 h, 86%; (b) **71**[12] (5.0 equiv), CH_2Cl_2, −78 to −30 °C, 3 h, 72%; (c) **67**[11] (1.0 equiv), Cs_2CO_3 (2.5 equiv), 2-dicyclohexylphosphino-2′,4′,6′-triisopropylbiphenyl (0.06 equiv), $PdCl_2(CH_3CN)_2$ (0.02 equiv), THF, 60 °C, 12 h, 80%; (d) $Ni(OAc)_2{\cdot}4H_2O$ (0.25 equiv), $NaBH_4$(0.25 equiv), ethylene diamine (1.0 equiv), EtOH, H_2, 23 °C, 12 h, 90%; (e) DMP (2.0 equiv), $NaHCO_3$ (4.0 equiv), CH_2Cl_2, 0 to 23 °C, 3 h, 80%; (f) $CrCl_2$ (7.0 equiv), CHI_3 (2.0 equiv), THF, −12 °C, 12 h, 55%; (g) HCl (4.0 M in dioxane, 2.0 equiv), MeOH, 23 °C, 1 h; (h) **62** (1.2 equiv), EDCI (1.5 equiv), HOAt (1.1 equiv), *i*-Pr_2NEt (3.0 equiv), CH_2Cl_2, 23 °C, 3 h, 61% over two steps; (i) TBAF (1.5 equiv), THF, 0 to 23 °C, 3 h, 83%; (j) $Pd(PPh_3)_4$ (0.25 equiv), CuI (1.0 equiv), DMF:Et_3N (2:1, *v*/*v*), 0 to 23 °C, 12 h, 29%; (k) HCl (4.0 M in dioxane, 2.0 equiv), MeOH, 23 °C, 1 h; (l) **20** (1.2 equiv), EDCI (1.5 equiv), HOAt (1.1 equiv), *i*-Pr_2NEt (3.0 equiv), CH_2Cl_2, 23 °C, 3 h, 65% over two steps; (m) TBAF (1.5 equiv), THF, 0 to 23 °C, 3 h, 88%; (n) $Pd(PPh_3)_4$ (0.25 equiv), CuI (1.0 equiv), DMF:Et_3N (2:1, *v*/*v*), 0 to 23 °C, 12 h, 31%; (o) Lindlar catalyst, quinoline, ethyl acetate, 23 °C, 8 h, 71%.

Designed disorazole B_1 analogue **9** with both of its two oxazole rings functionalized with an oxygenated residue was synthesized as shown in Scheme 4. Retrosynthetic analysis of this molecule based on the same general strategy relying on the symmetrical acetylene−vinyl iodide coupling/macrocyclization tactic required the substituted oxazole fragment **62**, whose

https://dx.doi.org/10.1021/jacs.0c07094
J. Am. Chem. Soc. XXXX, XXX, XXX−XXX

synthesis is summarized in Scheme 4A, and vinyl iodide fragment **63** [see Scheme 4B and Scheme 2C, conditions (n)].

The construction of required fragment **62** proceeded smoothly through a four-step sequence starting with readily available carboxylic acid **57**. Thus, **57** reacted with reagent **58**[10] to afford, in 83% yield, oxazole derivative **59** as shown in Scheme 4A. The latter was iodinated (LHMDS, 1,2-diodoethane, 86% yield) to afford iodo oxazole **60**, from which acetylene **61** was obtained through a Sonogashira coupling with TIPS-acetylene [$Pd(PPh_3)_4$ cat., CuI cat., 79% yield]. Cleavage of the TIPS group from TIPS-acetylene **61** ($LiOH{\cdot}H_2O$, 78% yield) finally led to the targeted fragment terminal acetylene **62**. Scheme 4B depicts the completion of the synthesis of targeted analogue **9**, starting with the coupling of vinyl iodide **63** (for preparation via **41**, see Scheme 2C) and carboxylic acid terminal acetylene **62**. Thus, reaction of **62** with iodide **63** in the presence of TCBC, Et_3N, and DMAP furnished ester **64** (45% yield). Subjecting the monomeric advanced intermediate **64** to the palladium/copper-catalyzed coupling/macrocyclization [$Pd(PPh_3)_4$ cat., CuI cat., 42% yield] led to macrocyclic bisacetylene precursor **65**, whose controlled hydrogenation with Lindlar catalyst/quinoline (64% yield) afforded the ultimate precursor **66**. Finally, exposure of the latter to H_2SiF_6 led to the desired analogue **9** in 65% yield, as shown in Scheme 4.

2.3. Synthesis of Bislactam Disorazole B_1 Analogues 10−12. Inspired by the clinically used anticancer drug Ixabepilone[6] (the lactam counterpart of epothilone B), disorazole B_1 analogues **10**, **11**, and **12** were designed and synthesized as summarized in Scheme 5. Based on the retrosynthetic analysis shown in Scheme 5A, the developed synthetic strategies defined the bisacetylene disorazole B_1 analogue **11** as the ultimate precursor from which disorazole B_1 analogue **12** could be generated through Lindlar hydrogenation. Precursor **11** and its modified oxazole counterpart **10** carrying a methyl-oxygenated side chain were then traced back to building blocks **20**, **62**, **67**,[11] and **68** as shown in Scheme 5A.

Scheme 5B summarizes the total synthesis of bislactam disorazole B_1 analogues **10**, **11**, and **12** starting with readily available aldehyde **69**.[3] Thus, sequential reaction of **69** with primary sulfonamide **70** in the presence of $Ti(OEt)_4$, followed by addition of Grignard reagent **71**[12] to the so-formed *N*-sulfonyl imine, gave secondary sulfonamide **72** (86% yield, single diastereoisomer). The configuration of the stereogenic centers within **72** were confirmed by X-ray crystallographic analysis of a downstream derivative (see below). Palladium-catalyzed coupling of acetylenic intermediate **72** with cyclopropyl iodide **67**[11] furnished hydroxy acetylene **73**, whose selective reduction [H_2, $Ni(OAc)_2{\cdot}4H_2O$, $NaBH_4$, 90% yield] led to (*Z*)-olefin **74**. Crystalline **74** [mp 96−98 °C, EtOAc:*n*-pentane (1:3, *v*/*v*)] yielded to X-ray crystallographic analysis[13] (see ORTEP representation of **74** in Scheme 5B). Oxidation of alcohol **74** (DMP, 80% yield) afforded aldehyde **68**, which was converted to (*E*)-vinyl iodide **75** through the action of CHI_3/$CrCl_2$ (55% yield). The latter was diverted along two different pathways toward lactam analogues **10** (pathway a), **11**, and **12** (pathway b), as depicted in Scheme 5B. Thus, exposure of **75** to HCl in dioxane liberated the corresponding amine, whose reaction with carboxylic acid fragment **62** in the presence of EDCI and HOAt afforded amide **76** in 61% overall yield. Desilylation of the latter (TBAF; 83% yield) gave ultimate precursor **77**, whose palladium/copper-catalyzed dimerization/macrocyclization furnished bislactam analogue **10** (29% yield), as shown in Scheme 5B. Intermediate **75** was then funneled through pathway b and toward analogues **11** and **12** as depicted in Scheme 5B. Thus, acid-induced cleavage (HCl in dioxane) of the sulfonamide moiety of **75**, followed by amide formation between the so-generated amine and oxazole carboxylic acid **20** (EDCI, HOAt), led to amide **78** in 65% overall yield for the two steps. Removal of the TBS group from **78** (TBAF, 88% yield), followed by dimerization/macrocyclization of the so-formed hydroxy vinyl iodide acetylene precursor under the influence of $Pd(PPh_3)_4$ cat. and CuI, furnished coveted lactam analogue **11** (31% yield). Finally, biscyclopropyl bislactam disorazole B_1 analogue **12** was generated from analogue **11** by Lindlar hydrogenation in the presence of quinoline, in 71% yield, as shown in Scheme 5 B.

2.4. Biological Evaluation of Disorazole B_1 and Analogues 3−12. Having secured synthetic disorazole B_1 (**2**, Figure 1) and its analogues **3**−**12** (Figure 2), their biological activities against uterine sarcoma cells (MES-SA), MES-SA cells with marked multidrug resistance due to overexpression of Pgp (MES-SA/Dx), and immortalized human embryonic kidney cells (HEK 293T) were evaluated with monomethyl auristatin E (MMAE) as a standard. Table 1 summarizes the results of these studies, and Figure 4 shows the structures of the most potent compounds discussed below. Thus, synthetic disorazole B_1 (**2**) exhibited single digit picomolar IC_{50} values against MES-SA (IC_{50} = 0.009 nM) and HEK 293T (IC_{50} = 0.003 nM) and subnanomolar potencies against MES-SA DX (IC_{50} = 0.32 nM). Interestingly, we could not find any previous cytotoxicity studies for disorazole B_1 (**2**) in the literature, making these findings, to our knowledge, the first report of the potent antitumor activities of disorazole B_1 (**2**). The biscyclopropyl disorazole B_1 analogue **3** also exhibited high potencies against MES-SA (IC_{50} = 0.059 nM) and HEK 293T (IC_{50} = 0.103 nM) but proved less potent against the drug-resistant MES-SA/Dx cell line (IC_{50} = 630.9 nM). From the remaining tested compounds, the bislactam analogues **11** and **12** proved to be the most potent, with **11** revealing the lowest IC_{50} values against all three cell lines (IC_{50} = 0.02 nM against MES-SA; IC_{50} = 0.01 nM against HEK 293T;

Table 1. Cytotoxicity Data Against Cell Lines MES-SA, MES-SA/Dx, and HEK 293T for Disorazole B_1 (2) and Disorazole Analogues 3−12[a]

compound	cell line		
	MES-SA[b] IC_{50} (nM)	MES-SA/Dx[c] IC_{50} (nM)	HEK 293T[d] IC_{50} (nM)
MMAE[e]	0.66	235.60	0.41
2	0.009	0.32	0.003
3	0.059	630.9	0.103
4	>20000	>20000	>20000
5	>20000	>20000	>20000
6	6.29	299.10	9.44
7	537.10	>20000	2264.00
8	>20000	>20000	>20000
9	>20000	>20000	>20000
10	16.97	>20000	45.14
11	0.02	0.71	0.01
12	0.23	3.18	0.27

[a]For details of the biological assays, see the Supporting Information. [b]Human uterine sarcoma cell line. [c]MES-SA cell line with marked multidrug resistance due to overexpression of Pgp. [d]Immortalized human embryonic kidney cell line. [e]Monomethylauristatin E.

https://dx.doi.org/10.1021/jacs.0c07094
J. Am. Chem. Soc. XXXX, XXX, XXX−XXX

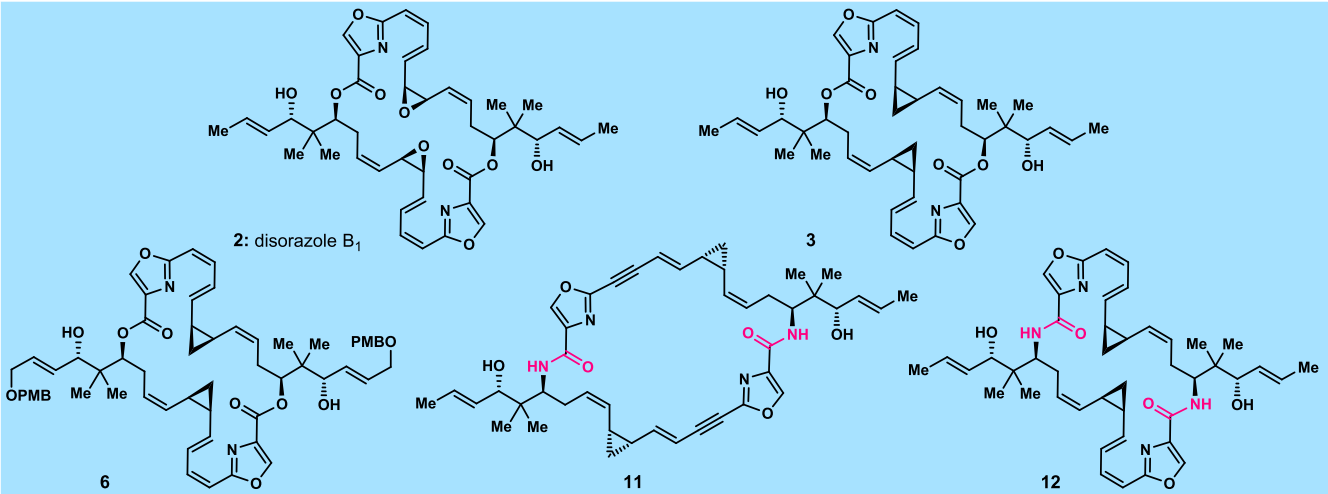

Figure 4. Potent disorazole B_1 analogues.

and IC_{50} = 0.71 nM against MES-SA/Dx). Analogue **12** also exhibited good potencies against all three cell lines tested (IC_{50} = 0.23 nM against MES-SA; IC_{50} = 0.27 nM against HEK 293T; and IC_{50} = 3.18 nM against MES-SA/Dx). Analogue **6**, equipped with the two PMB ether residues on its lipophilic wings, showed good activities against all three cell lines (IC_{50} = 6.29 nM against MES-SA; IC_{50} = 9.44 nM against HEK 293T; and IC_{50} = 299.10 nM against MES-SA/Dx). Particularly noteworthy are the high potencies of disorazole B_1 (**2**, IC_{50} = 0.32 nM) and analogues **11** (IC_{50} = 0.71 nM) and **12** (IC_{50} = 3.18 nM) against the multidrug-resistant cell line MES-SA/Dx. The described biological studies (with the three cell lines, as reported in Table 1) are the first step to a better understanding of the structure−activity relationships (SARs) and cytotoxicity properties of this class of compounds. More diverse and in-depth biological evaluations to decipher cytotoxicity against normal cells are expected later. However, these interesting results establish the first SARs within the disorazole B_1 (**2**) family of compounds (see summary in Figure 5), providing further guidance for future studies in the field.

3. CONCLUSION

Providing short and streamlined total syntheses to disorazole B_1 (**2**) and its analogues, the described chemistry opened new synthetic avenues to a variety of novel analogues of this naturally occurring molecule and resulted in the first structure−activity relationships (SARs) within this subclass of the disorazole B_1 compounds. Particularly interesting are the observations that the substitutions of the two epoxide moieties of disorazole B_1 with two cyclopropyl units lead to higher stability for the molecule while maintaining significant cytotoxic potencies [cf. IC_{50} values of compounds **2** and **3** (Figure 4), Table 1]. These investigations also revealed that substituting the two lactone moieties of disorazole B_1 for two lactam units also ensures significant cytotoxic properties of the molecule [cf. IC_{50} values of analogues **11** and **12** (Figure 4), Table 1], while they are expected to feature higher plasma stabilities than their bislactone counterparts. Analogue **6** (Figure 4), carrying the two extended oxygenated wings, maintains respectable potencies against the tested cell lines, pointing to tolerance of the disorazole B_1 scaffold to such modifications. Reported for the first time, the impressive potencies of disorazole B_1 (**2**) against the cell lines tested, especially the multidrug-resistant MES-SA/Dx cell line, elevate this molecule and its analogues to the front line as potential payloads for ADCs and possibly other applications as potential drugs alone or in combination with other drugs. These findings set the stage for further promising investigations aiming at novel payloads for antibody−drug conjugates[14] and/or small-molecule anticancer drugs, especially given the higher chemical stabilities of the newly synthesized compounds and their potent antitumor properties.

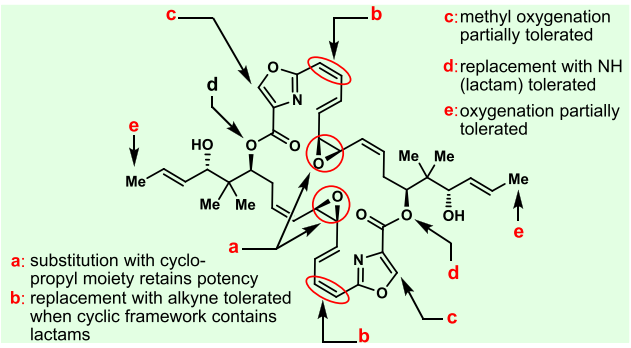

Figure 5. Structure−activity relationships of the synthesized disorazole B_1 analogues.

■ ASSOCIATED CONTENT

Supporting Information

The Supporting Information is available free of charge at https://pubs.acs.org/doi/10.1021/jacs.0c07094.

Experimental procedures and characterization data for all new compounds (PDF)

Crystallographic information for intermediate **74** (CIF)

■ AUTHOR INFORMATION

Corresponding Author

K. C. Nicolaou − *Department of Chemistry, BioScience Research Collaborative, Rice University, Houston, Texas 77005, United States;* orcid.org/0000-0001-5332-2511; Email: kcn@rice.edu

https://dx.doi.org/10.1021/jacs.0c07094
J. Am. Chem. Soc. XXXX, XXX, XXX−XXX

Authors

Johannes Krieger − *Department of Chemistry, BioScience Research Collaborative, Rice University, Houston, Texas 77005, United States*

Ganesh M. Murhade − *Department of Chemistry, BioScience Research Collaborative, Rice University, Houston, Texas 77005, United States*

Parthasarathi Subramanian − *Department of Chemistry, BioScience Research Collaborative, Rice University, Houston, Texas 77005, United States*

Balu D. Dherange − *Department of Chemistry, BioScience Research Collaborative, Rice University, Houston, Texas 77005, United States;* orcid.org/0000-0002-4123-5012

‖**Dionisios Vourloumis** − *Department of Chemistry, BioScience Research Collaborative, Rice University, Houston, Texas 77005, United States; Laboratory of Chemical Biology of Natural Products & Designed Molecules, Institute of Nanoscience and Nanotechnology, National Centre for Scientific Research "Demokritos", 153 10 Agia Paraskevi, Greece*

Stefan Munneke − *AbbVie Inc., South San Francisco, California 94080, United States*

Baiwei Lin − *AbbVie Inc., South San Francisco, California 94080, United States*

Christine Gu − *AbbVie Inc., South San Francisco, California 94080, United States*

Hetal Sarvaiaya − *AbbVie Inc., South San Francisco, California 94080, United States*

Joseph Sandoval − *AbbVie Inc., South San Francisco, California 94080, United States*

Zhaomei Zhang − *AbbVie Inc., South San Francisco, California 94080, United States*

Monette Aujay − *AbbVie Inc., South San Francisco, California 94080, United States*

James W. Purcell − *AbbVie Inc., South San Francisco, California 94080, United States*

Julia Gavrilyuk − *AbbVie Inc., South San Francisco, California 94080, United States*

Complete contact information is available at: https://pubs.acs.org/10.1021/jacs.0c07094

Notes

The authors declare no competing financial interest.

‖Dionisios Vourloumis unexpectedly passed away on March 21, 2020.

■ ACKNOWLEDGMENTS

We thank Drs. Lawrence B. Alemany and Quinn Kleerekoper (Rice University) for NMR spectroscopic assistance, Drs. Christopher L. Pennington (Rice University) and Ian Riddington (University of Texas at Austin) for mass spectrometric assistance, and Dr. Gary J. Balaich (University of California, San Diego) for the X-ray crystallographic analysis of compound **74**. This work was supported by AbbVie Stemcentrx, the Cancer Prevention & Research Institute of Texas (CPRIT), and The Welch Foundation (grant C-1819). K.C.N. is a CPRIT scholar in cancer research.

■ REFERENCES

(1) (a) Jansen, R.; Irschik, H.; Reichenbach, H.; Wray, V.; Höfle, G. Antibiotics from Gliding Bacteria, LIX. Disorazoles, Highly Cytotoxic Metabolites from the Sorangicin-Producing Bacterium *Sorangium Cellulosum* Strain So ce12. *Liebigs Ann. Chem.* **1994**, *1994*, 759−773. For a review on the disorazole family of compounds, see: (b) Hopkins, C. D.; Wipf, P. Isolation, Biology and Chemistry of the Disorazoles: New Anti-Cancer Macrodiolides. *Nat. Prod. Rep.* **2009**, *26*, 585−601.

(2) (a) Irschik, H.; Jansen, R.; Gerth, K.; Höfle, G.; Reichenbach, H. Disorazol A, an Efficient Inhibitor of Eukaryotic Organisms Isolated from Myxobacteria. *J. Antibiot.* **1995**, *48*, 31−35. (b) Carvalho, R.; Reid, R.; Viswanathan, N.; Gramajo, H.; Julien, B. The Biosynthetic Genes for Disorazoles, Potent Cytotoxic Compounds that Disrupt Microtubule Formation. *Gene* **2005**, *359*, 91−98. (c) Wipf, P.; Graham, T. H.; Vogt, A.; Sikorski, R. P.; Ducruet, A. P.; Lazo, J. S. Cellular Analysis of Disorazole C_1 and Structure−Activity Relationship of Analogs of the Natural Product. *Chem. Biol. Drug Des.* **2006**, *67*, 66−73. (d) Tierno, M. B.; Kitchens, C. A.; Petrik, B.; Graham, T. H.; Wipf, P.; Xu, F. L.; Saunders, W. S.; Raccor, B. S.; Balachandran, R.; Day, B. W.; Stout, J. R.; Walczak, C. E.; Ducruet, A. P.; Reese, C. E.; Lazo, J. S. Microtubule Binding and Disruption and Induction of Premature Senescence by Disorazole C_1. *J. Pharmacol. Exp. Ther.* **2009**, *328*, 715−722. (e) Elnakady, Y. A.; Sasse, F.; Lünsdorf, H.; Reichenbach, H. Disorazol A_1, a Highly Effective Antimitotic Agent Acting on Tubulin Polymerization and Inducing Apoptosis in Mammalian Cells. *Biochem. Pharmacol.* **2004**, *67*, 927−935.

(3) Nicolaou, K. C.; Bellavance, G.; Buchman, M.; Pulukuri, K. K. Total Syntheses of Disorazoles A_1 and B_1 and Full Structural Elucidation of Disorazole B_1. *J. Am. Chem. Soc.* **2017**, *139*, 15636−15639.

(4) Nicolaou, K. C.; Buchman, M.; Bellavance, G.; Krieger, J.; Subramanian, P.; Pulukuri, K. K. Syntheses of Cyclopropyl Analogues of Disorazoles A_1 and B_1 and Their Thiazole Counterparts. *J. Org. Chem.* **2018**, *83*, 12374−12389.

(5) For a dimerization approach toward disorazole C_1, see: (a) Ralston, K. J.; Ramstadius, H. C.; Brewster, R. C.; Niblock, H. S.; Hulme, A. N. Self-Assembly of Disorazole C_1 through a One-Pot Alkyne Metathesis Homodimerization Strategy. *Angew. Chem., Int. Ed.* **2015**, *54*, 7086−7090. For a review on biomimetic approaches toward dimeric natural products, see: (b) Stanley, P. A.; Spiteri, C.; Moore, J. C.; Barrow, A. S.; Sharma, P.; Moses, J. E. Biomimetic Approaches Towards The Synthesis of Complex Dimeric Natural Products. *Curr. Pharm. Des.* **2016**, *22*, 1628−1657.

(6) Lee, F. Y. F.; Borzilleri, R.; Fairchild, C. R.; Kim, S.-H.; Long, B. H.; Reventos-Suarez, C.; Vite, G. D.; Rose, W. C.; Kramer, R. A. BMS-247550: A Novel Epothilone Analog with a Mode of Action Similar to Paclitaxel but Possessing Superior Antitumor Efficacy. *Clin. Cancer Res.* **2001**, *7*, 1429−1437.

(7) For another total synthesis of a disorazole utilizing the Sonogashira reaction, see: Wipf, P.; Graham, T. H. Total Synthesis of (−)-Disorazole C_1. *J. Am. Chem. Soc.* **2004**, *126*, 15346−15347.

(8) (a) Schmid, C. R.; Bryant, J. D. D-(*R*)-Glyceraldehyde Acetonide. *Org. Synth.* **1995**, *72*, 6−8. (b) Zhao, Y.; Yang, T.; Lee, M.; Lee, D.; Newton, M. G.; Chu, C. K. Asymmetric Synthesis of (1′*S*,2′*R*)-Cyclopropyl Carbocyclic Nucleosides. *J. Org. Chem.* **1995**, *60*, 5236−5242.

(9) Nagao, Y.; Hagiwara, Y.; Kumagai, T.; Ochiai, M.; Inoue, T.; Hashimoto, K.; Fujita, E. New C4-Chiral 1,3-Thiazolidine-2-thiones: Excellent Chiral Auxiliaries for Highly Diastereocontrolled Aldol-Type Reactions of Acetic Acid and α,β-Unsaturated Aldehydes. *J. Org. Chem.* **1986**, *51*, 2391−2393.

(10) Ren, Z.-L.; Guan, Z.-R.; Kong, H.-H.; Ding, M.-W. Multifunctional Odorless Isocyano(triphenylphosphoranylidene)-Acetates: Synthesis and Direct One-Pot Four-Component Ugi/Wittig Cyclization to Multisubstituted Oxazoles. *Org. Chem. Front.* **2017**, *4*, 2044−2048.

(11) Inuki, S.; Ohta, I.; Ishibashi, S.; Takamatsu, M.; Fukase, K.; Fujimoto, Y. Total Synthesis of Cardiolipins Containing Chiral Cyclopropane Fatty Acids. *J. Org. Chem.* **2017**, *82*, 7832−7838.

(12) Reyes, J. R.; Winter, N.; Spessert, L.; Trauner, D. Biomimetic Synthesis of (+)-Aspergillin PZ. *Angew. Chem., Int. Ed.* **2018**, *57*, 15587−15591.

(13) CCDC-2011802 contains the supplementary crystallographic data for sulfinamide intermediate **74**. These data can be obtained free of charge from the Cambridge Crystallographic Data Centre, via www.ccdc.cam.ac.uk/structures.

(14) (a) Chari, R. V.; Miller, M. L.; Widdison, W. C. Antibody-Drug Conjugates: An Emerging Concept in Cancer Therapy. *Angew. Chem., Int. Ed.* **2014**, *53*, 3796−3827. (b) Nicolaou, K. C.; Rigol, S. Total Synthesis in Search of Potent Antibody−Drug Conjugate Payloads. From the Fundamentals to the Translational. *Acc. Chem. Res.* **2019**, *52*, 127−139. (c) Nicolaou, K. C.; Rigol, S. The Role of Organic Synthesis in the Emergence and Development of Antibody−Drug Conjugates as Targeted Cancer Therapies. *Angew. Chem., Int. Ed.* **2019**, *58*, 11206−11241.

https://dx.doi.org/10.1021/jacs.0c07094
J. Am. Chem. Soc. XXXX, XXX, XXX−XXX